

**TIME DOMAIN LOW FIELD NUCLEAR MAGNETIC RESONANCE FOR  
INVESTIGATING SILANE COUPLING IN A SILICA FILLED SBR MODEL  
TREAD COMPOUND**

By Jonathan E. Martens\*, Edward R. Terrill, and James T. Lewis  
Akron Rubber Development Laboratory, Inc., 2887 Gilchrist Rd, Akron, OH, USA

Richard J. Pazur  
Department of National Defense, Quality Engineering Test Establishment (QETE),  
Polymeric Materials & Advanced Textiles, Ottawa, ON, K1A 0K2 CANADA

Presented at the Fall 184th Technical Meeting of the  
Rubber Division of the American Chemical Society, Inc.  
Cleveland, OH  
**October 10, 2013**

ISSN: 1547-1977

\* Speaker

## Abstract

Time domain low field proton Nuclear Magnetic Resonance (NMR) was used to investigate the effect of silane coupling level in a model silica filled solution styrene-butadiene (SBR) rubber tire tread compound. Mechanical properties, crosslink density by volume swell and dynamic mechanical thermal analyses were also measured.

Two distinct families of NMR relaxation curves were observed depending on whether the system underwent vulcanization. Biexponential fitting of the relaxation provided the best confidence in the curve fitting parameters. The relative amount of the rigid lattice slowly decreases upon addition of the silane coupling agent in the unvulcanized compounds. Vulcanization causes an increase in the rigid lattice amplitude and a decrease in the short decay time due primarily to the crosslinking reactions. No noticeable trend in the NMR curve fitting parameters was detected as a function of coupling agent level in the vulcanized samples. However, the progressive increase in silane coupling concentration brought about a linear increase in modulus at 300% elongation, a decrease of  $\tan \delta$  (and rolling resistance) in the double strain sweep and a decrease in perceived crosslink density as measured by equilibrium volume swell. It is assumed that the crosslink density increase is due to the silane coupling reaction and that the NMR short decay results represents the total chemical crosslink density which remains constant. Combining these two observations together allowed the calculation of an average molar mass of interaction between the chains and the filler. In addition, a 33% increase over the optimal silane coupling agent concentration was beneficial for rolling resistance enhancement. A discussion is included about improving the experimental method and future investigations.

## Introduction

The advantages of using silica as a reinforcing agent in tire tread compounds are well documented<sup>1</sup>. The development of tires possessing long service life, driving safety and fuel economy has been enhanced with the introduction of bifunctional organosilanes which provide a chemical means of linking the silica and rubber together. Properties such as tensile strength, modulus, abrasion resistance and heat build up reduction due to hysteresis can be improved. Furthermore, chemical modification of the silica surface characteristics aids to lower filler-filler network attraction which is beneficial for improved compound processability. Moreover, the use of silica fillers is paramount in achieving the desired combination of wet traction versus rolling resistance in tire tread compounds<sup>2</sup>.

Low field <sup>1</sup>H solid-state Nuclear Magnetic Resonance (NMR) is a well established spectroscopic technique employed to analyze the amount of chain restrictions or constraints present in filled rubber systems<sup>3</sup>. The most often used method involves the measurement of the transverse  $T_2$  spin-spin relaxation by using a Hahn-Echo (HE) or Carr-Purcell-Meiboom-Gill pulse sequence. The process of NMR relaxation due to the decay of the proton magnetization from the maximum of the spin echo is correlated to the

polymer chain mobility. Besides chemical crosslinks, chain mobility can be reduced by temporary physical chain entanglements, trapped chain entanglements due to vulcanization, and filler effects (i.e. absorbed chains on active filler surfaces). Plasticizers appear to lessen the amount of perceived chain entanglements<sup>4</sup>.

Many research papers deal with studying the nature of silica-elastomer interactions by using low field NMR techniques<sup>5-14</sup>. As in the case of other particulate fillers such as carbon black, different molecular mobilities have been identified pertaining primarily to the bound *versus* unbound (or bulk) rubber regions. Chain dynamics vary in relationship to the silica-elastomer interface. Chains that interact with the active surface possess the lowest mobility causing the apparition of a so-called glass transition gradient extending into the bulk phase<sup>5</sup>. In an unvulcanized natural rubber/silica model system, the immobilized layer was identified as rubber chains and coupling agent molecules on the silica surface, while network chains and physically absorbed chains were in an intermediate mobility zone<sup>6</sup>. The highest amount of immobilized chains occurred in pure silica while chemical coupling was found to decrease the proportion of these chains. From the bound rubbers extracted from silica filled poly(isoprene) and *cis*-poly(butadiene), two relaxation times corresponding to the tightly and loosely bound rubber were measured<sup>7</sup>. By HE NMR, the density of network junctions increases with the increasing silica content in SBR<sup>8,9</sup>. The use of Multiple Quantum (MQ) techniques can negate the filler effect on the total NMR relaxation<sup>9</sup>.

Other investigations using experimental techniques such as dynamic mechanical analyses (DMA) and differential scanning calorimetry (DSC) that probe the glass transition temperature have found no evidence for reduced segmental mobility near the silica surface in SBR<sup>15</sup>. In fact, there is some doubt that the NMR relaxation technique and subsequent curve fitting of the parameters are providing real data related to polymer mobility at the polymer/filler interface<sup>16</sup>.

We have been studying the dynamic behavior of a model silica filled solution SBR compound for use in tire treads<sup>17,18</sup>. These studies have confirmed that functionalization of the SBR preferentially lowers  $\tan \delta$  thus reducing rolling resistance and improving fuel economy. It is thought that additional favorable interactions between the chains (backbone and chain end modified) and the silica are responsible for decreasing hysteretic effects<sup>18,19</sup>. Other functionalized solution SBRs providing similar advantages in tire properties have been investigated by other groups as summarized in ref. 20. Both the hysteresis and the Payne effect were lessened due to the lowering of the number of free polymer chain ends by their absorption and reaction with active filler surface.

The influence of the silane coupling agent concentration upon silica/chain interactions by time domain NMR for a model silica filled solution SBR compound will be investigated. Silane coupling agent concentrations will be varied from 0 to 133% of its optimal concentration. The mixing procedure will be the same for all compounds to ensure compound consistency. Besides NMR, tensile and dynamic mechanical testing (DMTA) to predict tire performance will also be carried out. Correlations between the different test methods will be also be carried out.

## Experimental

### *Compounds and Mixing Procedure*

The five compounds identified in Table 1 were mixed in three stages in accordance to the procedure outlined in Table 2. Detailed ingredient descriptions are provided in the appendix. A silane coupling concentration of 5.2 phr (compound D) was considered as the optimal concentration (100%) assuming a ratio of silica/coupling agent of 12.5. Two levels below this concentration (B and C) and one above (E) were added in order to probe an expanded range of coupling agent levels. Compound A does not contain any coupling agent.

| Ingredient                         | Compound Identification |              |              |              |              |
|------------------------------------|-------------------------|--------------|--------------|--------------|--------------|
|                                    | A                       | B            | C            | D            | E            |
| <b>Silane Coupling Agent Level</b> | <b>0%</b>               | <b>33%</b>   | <b>67%</b>   | <b>100%</b>  | <b>133%</b>  |
| <b>STAGE 1</b>                     |                         |              |              |              |              |
| F-S-SBR                            | 75                      |              |              |              |              |
| PB                                 | 25                      |              |              |              |              |
| Carbon black                       | 15                      |              |              |              |              |
| Silica                             | 65                      |              |              |              |              |
| Silane Coupling Agent              | 0                       | 1.7          | 3.5          | 5.2          | 6.9          |
| Aromatic Oil                       | 24                      |              |              |              |              |
| Stearic acid                       | 1.5                     |              |              |              |              |
| <b>Masterbatch 1</b>               | <b>205.5</b>            | <b>206.8</b> | <b>208.1</b> | <b>209.4</b> | <b>210.7</b> |
| <b>STAGE 2</b>                     |                         |              |              |              |              |
| Zinc oxide                         | 1.9                     |              |              |              |              |
| Wax                                | 2                       |              |              |              |              |
| A/O 1                              | 2                       |              |              |              |              |
| A/O 2                              | 0.5                     |              |              |              |              |
| <b>Masterbatch 2</b>               | <b>211.9</b>            | <b>213.2</b> | <b>214.5</b> | <b>215.8</b> | <b>217.1</b> |
| <b>STAGE 3</b>                     |                         |              |              |              |              |
| Sulfur                             | 1.05                    |              |              |              |              |
| CBS                                | 0.91                    |              |              |              |              |
| DPG                                | 1.05                    |              |              |              |              |
| <b>Total Phrs</b>                  | <b>214.9</b>            | <b>216.2</b> | <b>217.5</b> | <b>218.8</b> | <b>220.1</b> |

**Table 1:** Chemical compositions of the five silica based SBR compounds

Mixing took place on a Farrel BR laboratory size mixer. Rotor speed was increased during stages 1 and 2 at the 4.5' and 3.5' marks in order to reach the desired hold temperature. The third stage drop temperature was reached after about 2.5 minutes. The mixed rubber was sheeted out three times on a two roll mill after completion of each stage.

| Stage | Rotor speed (rpm) | Temperature (°C) | Ram Pressure (psi) | Hold time (min) | Hold and Drop Temperature (°C) |
|-------|-------------------|------------------|--------------------|-----------------|--------------------------------|
| 1     | 65                | 65               | 50                 | 2               | 160                            |
| 2     | 65                | 65               | 50                 | 4               | 140                            |
| 3     | 60                | 50               | 50                 | 0               | 110                            |

**Table 2:** Mixer and mixing conditions during the three stages of compound mixing.

### *Test Procedures*

Room temperature tensile properties were measured using die C dumbbell specimens according to ASTM D412.

Double Strain Sweeps in the tensile mode were carried out on a Metravib +150 Dynamic Mechanical Thermal Analyser (DMTA) at 10Hz and 30°C. Second sweep results are presented.

The determination of the chemical crosslink density of the five compounds was carried out by performing equilibrium solvent swell measurements followed by use of the modified Flory Rehner equation assuming crosslink fluctuations (i.e. phantom network) and a functionality of four.

$$\ln(1 - v_r) + v_r + \chi v_r^2 = -\frac{\rho}{2M_{c,sw}} V_s v_r^{\frac{1}{3}} \quad (1)$$

In equation 1,  $V_s$  is the molar volume of the swelling solvent,  $v_r$  is the volume fraction of rubber in the swollen state and  $\chi$  is the Flory Huggins polymer-solvent interaction parameter. A  $\chi$  value of 0.413 (in toluene) was used in order to estimate  $M_{c,sw}$ , the average molecular weight between crosslinks (chemical crosslinks and trapped entanglements together) for the SBR rich compounds<sup>18</sup>. This method assumes the disentanglement of the polymers chains during swelling in the good solvent.

A Bruker model mini-spec time domain NMR apparatus was employed to measure spin echo relaxation data for the unvulcanized and vulcanized compounds. A resonance frequency of 20 MHz and test temperature of 363K were used. The standard Hahn-Echo pulse sequence (90°/t/180°/t(acquisition up to 200ms)) was employed using 32 scans and a recycle delay of 0.5s. Each compound was tested in triplicate and the resulting curve fitting data were averaged.

A linear combination of exponential decay functions will be used to model the decrease in magnetization ( $M(t)$ ) of the rubber compounds:

$$\frac{M(t)}{M_0} = A \exp\left(\frac{-t}{T_{21}}\right) + B \exp\left(\frac{-t}{T_{22}}\right) + C \quad (2)$$

The decay times of the rigid (chemical crosslinks and physical entanglements) and mobile (dangling chain ends) phases are given by  $T_{21}$  and  $T_{22}$  respectively. The amplitude values of  $A$ ,  $B$  and  $C$  reflect the relative amount of proton magnetization of the rigid, dangling chain end and highly mobile sol fractions. Curve fitting software (Jump software) was used for equation verification and subsequent calculations and analyses in order to provide confidence in the NMR parameters. Needless to say, the curve fitting analysis is not without error and can lead to misinterpretation<sup>16, 21, 22</sup>.

The number average molar mass between crosslinked chains ( $M_{c,NMR}$ ) is directly proportional to the fast decay component of the relaxation:

$$M_{c,NMR} \propto T_{21} \quad (3)$$

This same relationship can be applied to estimate the number average molar mass between physical chain entanglements ( $M_e$ ) for the gum and unvulcanized compound. In the usual case of tetrafunctional crosslinking in rubber systems, a chemical crosslink density ( $\nu_c$ ) may be calculated by using  $\nu_c = \rho/2M_c$  where  $\rho$  is the density of the elastomer.

## Results and Discussion

A summary of the mechanical properties of the five compounds is presented in Figures 1 and 2. Without silane coupling, the stress strain curve displays lower moduli and the highest elongation to break due to the lack of compatibility between the silica surface and the polymer chains. Upon its progressive addition, mechanical properties improve as witnessed by an increase in both higher strain moduli and the tensile strength. A general decrease in elongation to break is noted. The modulus at 300% elongation, which is commonly used to measure the extent of silica/chain coupling effects, demonstrates an excellent correlation with increasing silane coupling concentration. Tensile strength on the other hand, shows less of a correlation and less of a change of value. The 67 and 100% stress strain curves are demonstrating quite similar mechanical behavior while the 133% curve suggests an improvement over the properties of the optimized formulation. This series of stress strain curves provide evidence that chemical coupling has taken place between the polymer unsaturation and the silica surface.

The double strain sweep plots of Fig. 3 provide a combination of the Payne (elastomer-filler interactions) and Mullin's (stress softening) effects. In the region of particular interest from 0.01 to 0.1 dynamic strain, the general trend is a decrease in  $\tan \delta$  signifying that rolling resistance is enhanced upon addition of the coupling agent. In other words, less of the filler-polymer network is destroyed under the action of dynamic strain. Compound E which represents 133% of the optimum coupling agent concentration, is displaying the lowest  $\tan \delta$  in the dynamic strain region of interest for tire rolling

resistance. This particular finding corroborates with the mechanical property test results. Chemical coupling by the silane coupling is responsible for the improvement in properties along with a reduction in filler-filler interactions.

The unvulcanized and vulcanized NMR relaxation curves have been plotted in Fig. 4. Two families of curves are in evidence showing the effect of vulcanization on the HE response in the acquisition region of approximately 0.3 to 20 ms which is sensitive to the chemical crosslinking and dangling chain end behavior. Furthermore, the unvulcanized curves in this critical region appear to display more variation while the vulcanized ones superimpose onto one curve as a function of silane coupling agent concentration. These contrasting observations will be discussed later on in the data analysis section.

Different curve fitting strategies (combinations of exponential and Gaussian-exponential) were attempted, but it was found that a biexponential fit (eq. 2) of the relaxation data provided excellent curve fitting ( $R^2 = 0.9999$ ) and that the total error of the magnetization amplitudes and time constants were minimized. A typical curve fitting result including residuals is provided in Fig. 5 for the unvulcanized compound A. The C fraction of equation 2 was eliminated from the calculations as its values were very low (0.3 to 0.4 %) for all compounds.

A table of the calculated NMR curve fitting parameters is given for the unvulcanized and vulcanized compounds in Table 3. Amplitude values for the unvulcanized compounds appear to display a possible trend: the value of A appears to decrease slightly with increasing coupling agent concentration while conversely, the magnitude of B increases in this same interval. These observations have been captured in Fig. 6 and are supported by the relaxation curves presented in Fig. 4. The progressive insertion of the coupling agent acts to lower the overall rigidity of the network chains (increased mobility due to lubrication) by increasing the mobility of the free chain ends. In addition, the fast decay  $T_{21}$  appears to slowly increase as a function of silane coupling addition but scatter is apparent. The lowering of the magnitude of the rigid portion can be explained by the presence of both the reacted and unreacted silane coupling agent. Reaction of the one end of the coupling agent with the silica surface has modified its surface characteristics rendering it less hydrophilic towards the SBR (and BR) polymer chains. This initial reaction is also believed to improve the filler-filler dispersion which will aid in limiting the flocculation process during vulcanization. Any unreacted or free silane coupling agent will behave as a “sol” type molecule and may be responsible for the increased mobility of the free chain ends.

|                     | A    | B    | C    | D    | E    |
|---------------------|------|------|------|------|------|
| <b>Unvulcanized</b> |      |      |      |      |      |
| A                   | 82.6 | 82.4 | 82.0 | 80.5 | 80.3 |
| T <sub>21</sub>     | 2.54 | 2.50 | 2.56 | 2.72 | 2.63 |
| B                   | 17.4 | 17.6 | 18.0 | 19.5 | 19.7 |
| T <sub>22</sub>     | 26   | 25   | 26   | 26   | 25   |
| <b>Vulcanized</b>   |      |      |      |      |      |
| A                   | 83.6 | 83.8 | 84.4 | 83.9 | 83.9 |
| T <sub>21</sub>     | 2.20 | 2.14 | 2.11 | 2.20 | 2.17 |
| B                   | 16.4 | 16.2 | 15.6 | 16.1 | 16.1 |
| T <sub>22</sub>     | 27   | 27   | 26   | 28   | 28   |

**Table 3:** Summary of the NMR curve fitting parameters for the unvulcanized and vulcanized compounds. A and B amplitudes have been normalized to 100%.

Vulcanization of the system brings about huge changes in the curve fitting data. The A amplitude increases by 3-4% at the expense of the proportion of dangling chain ends. Values of T<sub>21</sub> decrease by about 0.4-0.5 ms on average across the five compounds while values of T<sub>22</sub> increase from 1 to 3 ms. Such observations in the fitting data are normally observed during vulcanization during which in this case, sulfur linkages are produced between adjacent polymer chains providing a crosslinked and rigid lattice network (hence, the increase in the A value). The reaction and incorporation of the vulcanization ingredients like sulfur into the network would allow for a decrease in the B fraction (which also includes sol type highly mobile molecules). Perhaps the most surprising result is that no significant difference between all four curve fitting parameters is observed from the vulcanized compounds A to E (see also Fig. 6). At first sight, this observation suggests the predominance of the chemical crosslinking reactions, providing a relatively constant crosslink density in the five compounds. Additional chain restrictions as caused by the linking of the silane coupling agent with the unsaturation in the polymers which was expected to be seen by a lowering of T<sub>21</sub> were not observed. However, amplitude values of A and B do become more constant for the five compounds upon vulcanization suggesting that the silane coupling agent has changed into a less mobile chemical form compared to the unvulcanized state. To say the least, this is still weak and indirect evidence extracted from the NMR curves to support the chemical coupling reaction.

It was immediately suspected that timescale of NMR data acquisition may be the cause in not directly detecting the silane coupling reactions, in particular with the polymer unsaturation. The expanded region in the 0.1 to 0.3 ms of the vulcanized samples in Fig 7 shows that the data points and curves are not illustrating any significant trend as a function of silane coupling agent concentration. Any deviation in the experimental values is due to scatter. Since the coupling reaction with the chain unsaturation is taking place near the silica surface in the zone of bonded rubber, it is likely that other pulse sequences may be necessary to extract this chain restriction information in the less mobile or rigid

phase<sup>6,23</sup>. The use of monodisperse spherical silica particles produced by the Stöber process is reported to aid in defining a model interface to probe molecular mobility on the silica surface. It has also been noted that the styrene unit relaxation of SBR may interfere with the relaxation of the rubber/silica interface resulting in confusion with the data interpretation<sup>6</sup>.

Equilibrium volume swell coupled with the Flory-Rehner analysis by eq. 1 provided chemical cross link data (chemical crosslinks + trapped chain entanglements) for the five vulcanized compounds. These data were plotted against the modulus and elongation to break in Fig. 8. The modulus at 300% displays a good correlation, increasing in value with the chemical crosslink density measurements. On the other hand, the elongation to break provided a poorer correlation, but showed a modest decrease with increasing crosslink density. Assuming that combined chemical crosslink and trapped chain entanglement density is constant through the five compounds (the NMR  $T_{21}$  values were constant), it is likely that the additional silane coupling to the polymer unsaturation is responsible for the perceived increase in total chemical crosslink density. In this case, assuming that it is possible to decouple the chemical crosslinks (+ trapped chain entanglements) from the additional filler-chain reactions, one can estimate that,

$$\frac{1}{M_{c,sw}} \approx \frac{1}{M_c} + \frac{1}{M_{chain-filler}} \quad (4)$$

where  $M_c$  represents only the chemical crosslink and trapped chain entanglements molecular weights.

Reported values of  $M_e$  for SBR containing 23.5% styrene vary from 3-3.2 kg/mol<sup>20</sup> while for *cis*-poly(butadiene), the measured value is 2.3 kg/mol<sup>24</sup>. Given a 75/25 blend of SBR/PB in the tread compound, we will assume inverse linear additivity in the entanglement density values in the compound and use an averaged value of 2.8 kg/mol to represent the average molecular weight between entanglements. Given the values of  $T_{21}$  for the unvulcanized and vulcanized compounds in table 3 along with the relationship of eq. 3, an estimated value of  $M_{c, NMR}$  for all the compounds is 2.3 kg/mol. This is an approximative value since the value of  $T_{21}$  for the unvulcanized SBR contains relaxation contributions from the silica-rubber interface, the poly(butadiene) and from the plasticizer. Assuming that this derived value of  $M_c$  by NMR pertains only to the linear combination of chemical crosslinks, trapped entanglements and free chain entanglements, it is possible to write:

$$\frac{1}{M_{c,NMR}} \approx \frac{1}{M_c} + \frac{1}{M_e} \quad (5)$$

It can be readily seen that combining equations 4 and 5 provides a means to estimate the magnitude of  $M_{chain-filler}$ . These values are plotted in Figure 9 as a function of silane coupling agent level. The magnitude of  $M_{chain-filler}$  decreases in a regular and linear fashion with the addition of silane coupling agent. This can be attributed to its reaction

with the rubber unsaturation during vulcanization. The value of  $M_{\text{chain-filler}}$  for no coupling agent can be related to the interactions taking place between the polymer chains with the silica surface. In addition, an improvement in chain-filler interaction appears beyond the 100% optimal level of silane coupling agent. This observation agrees with the tensile and dynamic testing results.

More work is required to understand the filler-rubber interactions, in particular in the challenging case of silica and SBR. The use of a model tread compound made NMR result interpretation that much more complex due to the blend component, the inclusion of some carbon black and the high loading of aromatic plasticizer. Moreover, the functionalization of the SBR polymer backbone and chain ends and their effect on interactions with the silica surface was not thoroughly investigated by NMR given the lack of a control conventional SBR. Further studies on these topics will be presented in subsequent investigations.

## Conclusions

Two distinct families of NMR relaxation curves for the five model compounds were observed depending on whether the system was vulcanized. Biexponential fitting of the relaxation provided the best confidence in the curve fitting parameters. The magnitude of the rigid lattice slowly decreases upon addition of the silane coupling agent in the unvulcanized state. Vulcanization causes an increase in the rigid lattice amplitude and a decrease in the short decay time due primarily to the crosslinking reactions. No noticeable trend in the NMR curve fitting parameters was detected as a function of coupling agent level in the vulcanized samples. However, the progressive increase in silane coupling concentration brought about a linear increase in modulus at 300% elongation, a lower  $\tan \delta$  (and rolling resistance) and a decrease in perceived crosslink density as measured by equilibrium volume swell. It is assumed that the crosslink density increase is due to the silane coupling reaction and that the NMR short decay results suggest a constant total chemical crosslink density. Combining these two observations together allowed the measurement of an average molar mass of interaction between the chains and the silica filler. A 33% increase over the optimal silane coupling agent concentration was beneficial for rolling resistance enhancement. A discussion is included about improving the experimental method and future investigations.

## References

1. S. Wolff in “The Major International Tyre Technology Conference – Book of Papers“, Rapra Technology Ltd., Shrewsbury, UK (1993)
2. S. Futamura, K-C. Hua, Rubber World, September, 17 (2010).
3. “Spectroscopy of Rubber and Rubbery Materials“ Eds. V.M. Litvinov, P.D. Prajna, Rapra Technology Ltd., Shrewsbury, UK, 353 (2002)
4. R.J. Pazur, D. Lee, F.J. Walker, M. Kasai, RUBBER CHEM. TECHNOL. **85**, 295 (2012).
5. J.L. Valentin, I. Mora-Barrantes, J. Carretero-Gonzalez, M.A. Lopez-Manchado, P. Sotta, D.R. Long , K. Saalwächter, *Macromolecules* **43**(1), 334 (2010).
6. J.W ten Brinke, V.M. Litvinov, J.E.G.J. Wijnhoven, J.W.M. Noordermeer, *Macromolecules* **35**(27), 10026 (2002).
7. Ito M., Nakamura T., and Tanaka K. *Journal of Applied Polymer Science* **30**, 3493 (1985).
8. H. Luo, M. Klüppel, H. Schneider, *Macromolecules* **37**, 8000 (2004).
9. K. Saalwächter, M. Klüppel, H. Schneider, *Appl. Magn. Reson.* **27**, 401 (2004).
10. Ono S., Kiuchi Y., Sawanobori J., Ito M. *Polymer International* **48**, 1035 (1999).
11. I. Mora-Barrantes, J.L. Valentin, P. Posadas, A. Marcos, A. Rodriguez , L. Ibarra, L. Gonzalez, 176<sup>th</sup> ACS Rubber Division Meeting, paper 96 (2009).
12. J-H. Ma, L-Q. Zhang, Y-P. Wu, *Journal of Macromolecular Science, Part B: Physics* **52**(8), 1128 (2013).
13. J. Berriot, F. Martin, H. Montes, L. Monnerie, P. Sotta, *Polymer* **44**(5), 1437 (2003).
14. M. Gussoni, F. Greco, M. Mapelli. A. Vezzoli. E. Ranucci. P. Ferruti, Zetta, L., *Macromolecules*, **35**, 1722 (2002).
15. C.G. Robertson, C.J. Lin, R.B. Bogoslovov, M. Rackaitis, P. Sadhukhan, J.D. Quinn, C.M. Roland, RUBBER CHEM. TECHNOL. **84**, 507 (2011).
16. C.G. Robertson, C.M. Roland, RUBBER CHEM. TECHNOL. **81**, 506 (2008).
17. J.E. Martens, E.R. Terrill, J.T. Lewis, 180<sup>th</sup> ACS Rubber Division Meeting, paper 71 (2011).
18. J. E. Martens, E. R. Terrill, J. T. Lewis, R. J. Pazur, R. Hoffman, 182<sup>nd</sup> ACS Rubber Division Meeting, paper 67 (2012)
19. S.K.H. Thiele, D. Bellgardt, 176<sup>th</sup> ACS Rubber Division Meeting, paper 150, (2009).
20. W.L. Hergenrother, J.D. Ulmer, C.G. Robertson , RUBBER CHEM. TECHNOL. **79**, 338 (2006).
21. Saalwächter, K., *Macromolecules* **38**, 1508 (2005).
22. R.J. Pazur, F.J. Walker, *Kautsch. Gummi Kunstst.*, **64**,16 (2011).
23. A. Papon, K. Saalwächter, K. Schäler, L. Guy, F. Lequeux, H. Montes, *Macromolecules* **44**, 913 (2011).
24. L.J. Fetters, D.J. Lohse, R.H. Colby in *Physical Properties of Polymers Handbook*, Ed, J.E. Mark, American Institute of Physics Press, Woodbury, NY, p. 335 (1996).

## Appendix

| Ingredient            | Trade name        | Description  | Supplier       |
|-----------------------|-------------------|--|----------------|
| F-S-SBR               | Sprintan SLR-4602 | Tin coupled F-S-SBR, 37.5phr TDAE, high vinyl (67% of BD), 25% S | Styron         |
| PB                    | Budene 1207       | cis 1-4 Poly(butadiene) (97% cis 1-4 content)                    | Goodyear       |
| Carbon black          | N234              | Carbon Black   |                |
| Silica                | Ultrasil 7000 GR  | Silica   |                |
| Silane coupling agent | Si266             | Bis(triethoxysilylpropyl)polysulfide                             | Evonik         |
| Aromatic oil          | Aromatic Oil      | Sundex 790   | Holly Refinery |
| Stearic Acid          | stearic acid      | Fatty acid   |                |
| Zinc Oxide            | zinc oxide        | Cure activator   |                |
| Wax                   | Okerin wax 7240   | microcrystalline wax   |                |
| A/O 1                 | Santoflex 6PPD    | 6PPD   |                |
| A/O 2                 | Wingstay 100      | diphenyl p-phenylene diamine                                     |                |
| Sulfur                | Sulfur            | Cross-linker   |                |
| CBS                   | Santocure CBS     | Accelerator  |                |
| DPG                   | Perkacit DPG-grs  | Accelerator  |                |

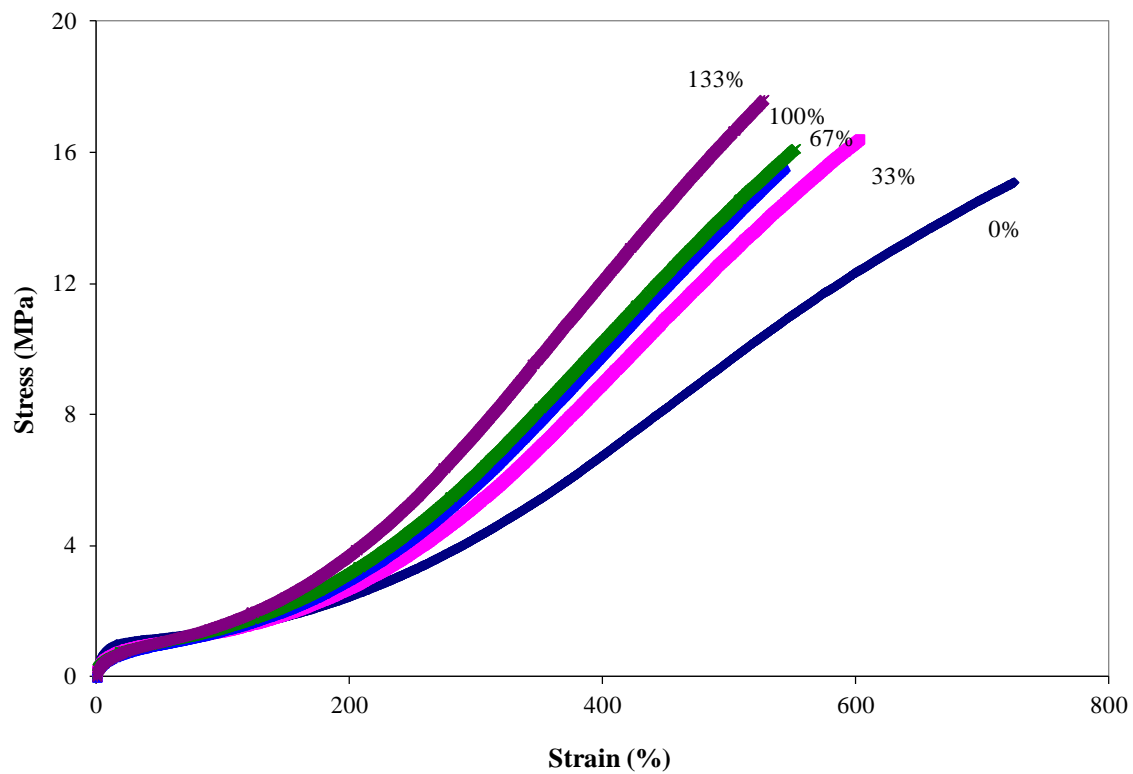


FIG. 1 – Stress-Strain curves of the SBR compounds as function of silane coupling agent concentration (N.B. 100% = 5.2 phr)

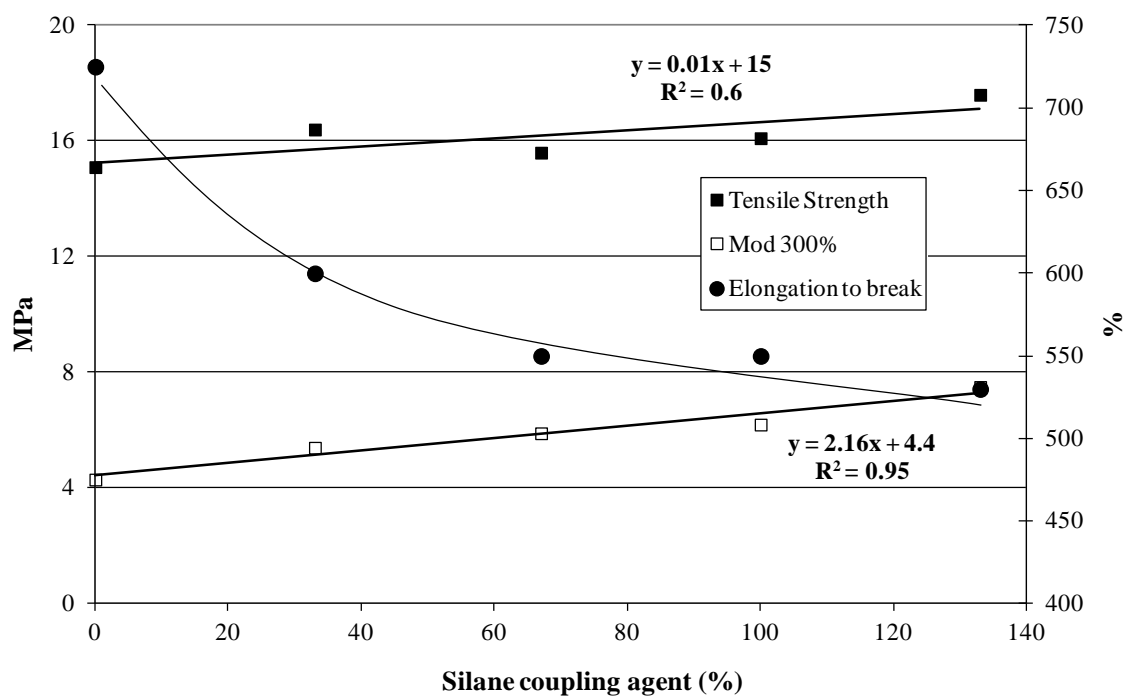


FIG. 2 – Selected mechanical properties plotted against silane coupling agent level.

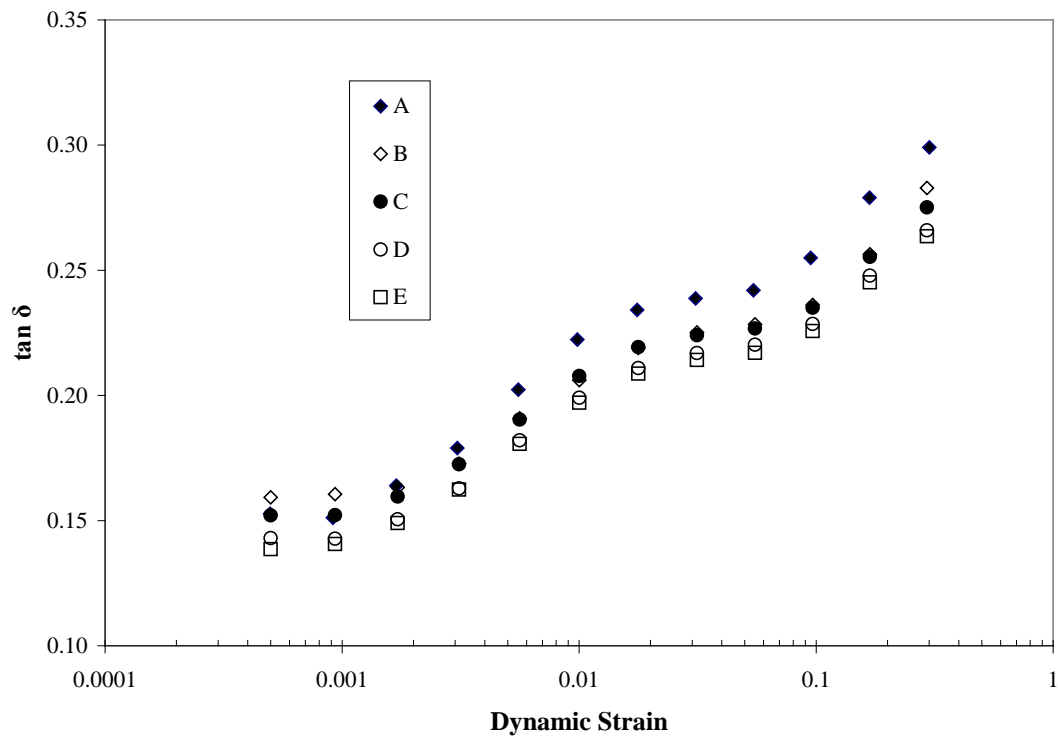


FIG. 3 – Double strain sweep results for rolling resistance performance (30°C).

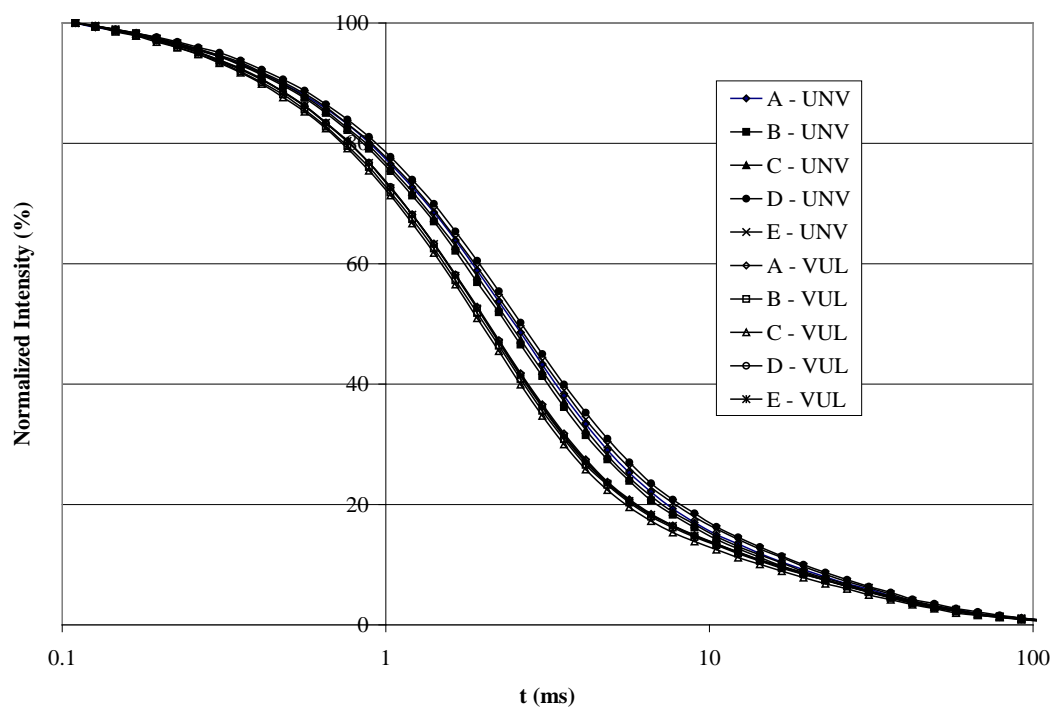


FIG. 4 – NMR relaxation curves representing the unvulcanized (UNV) and vulcanized (VUL) compounds.

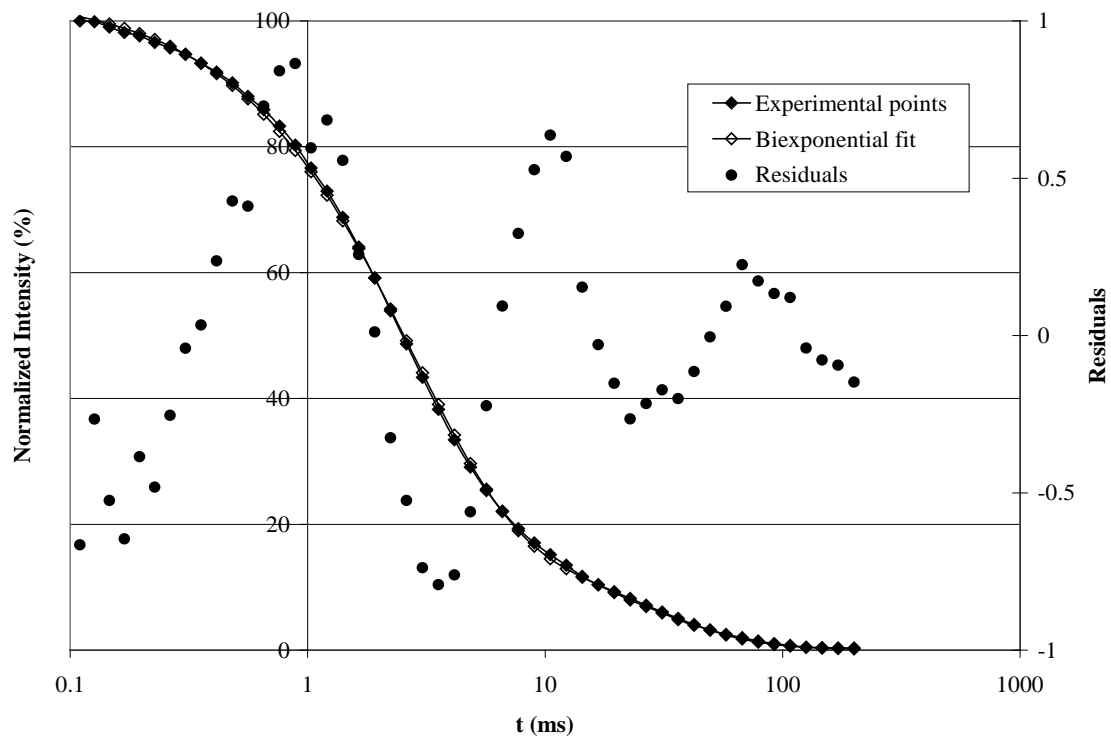


FIG. 5 – Example of biexponential curve fit for the relaxation data of Compound A ( $R^2 = 0.9999$ ).

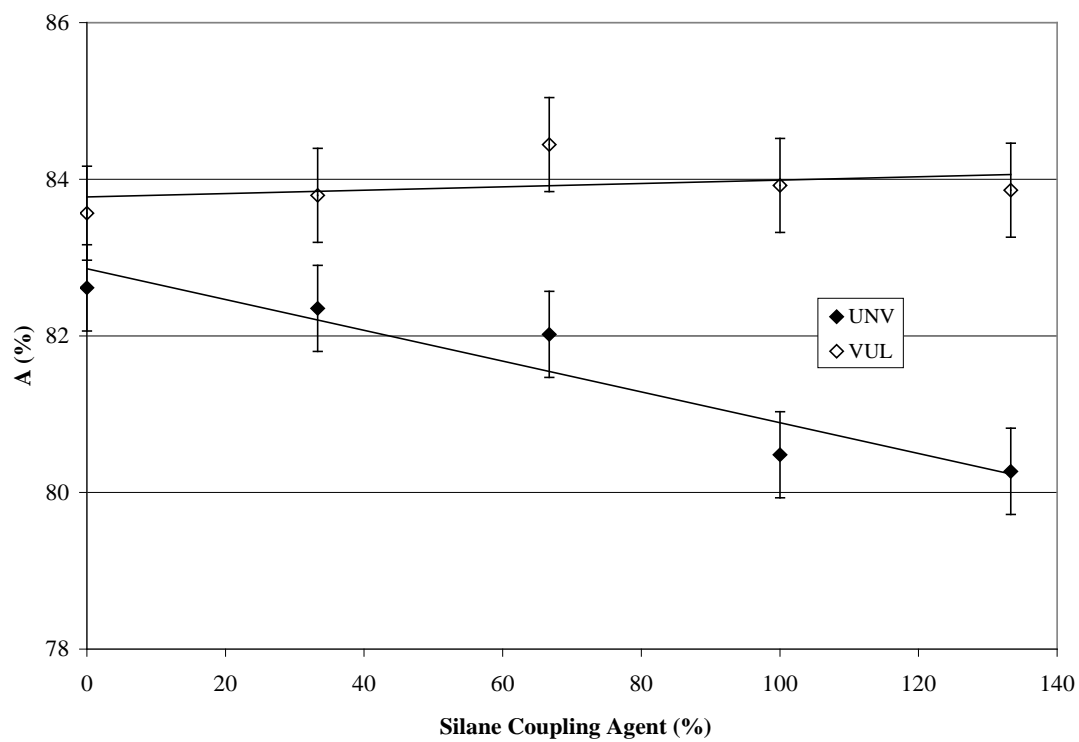


FIG. 6 – Amplitude of the rigid chain lattice for the unvulcanized and vulcanized compounds.

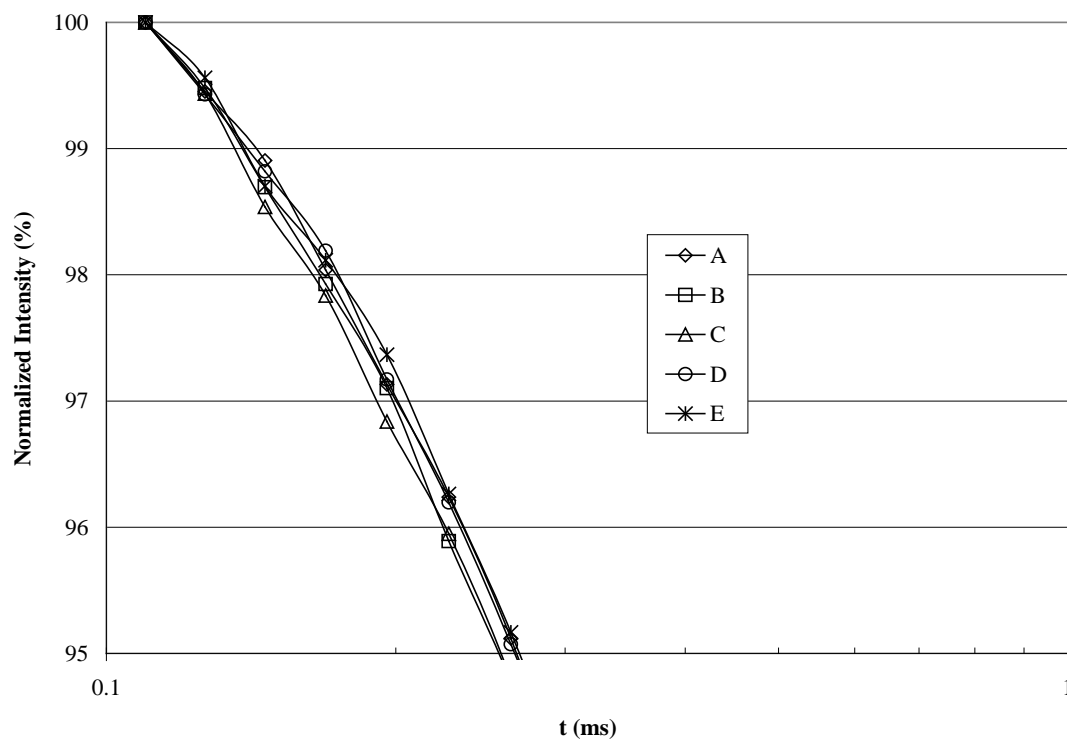


FIG. 7 – Closeup of the short acquisition time region for the NMR relaxation curves of the vulcanized samples.

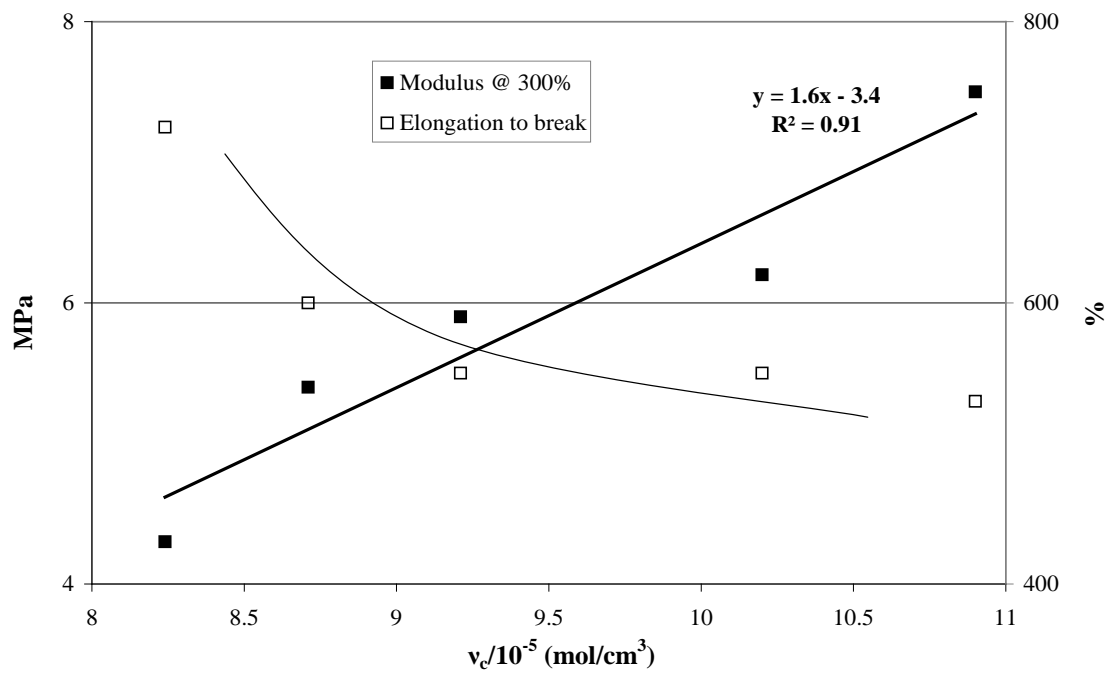


FIG. 8 – Modulus at 300% and elongation at break *versus* chemical crosslink density by volume swell.

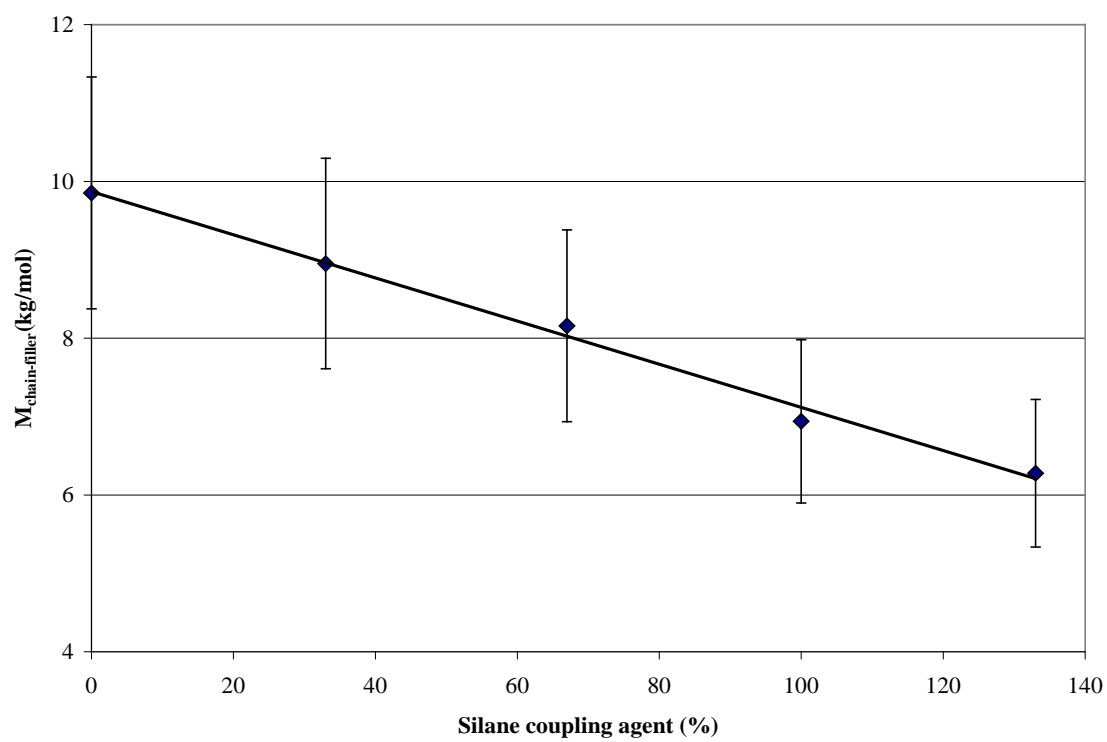


FIG. 9 –Values of the mean molar mass quantifying the interactions between the chains and the fillers.(15% estimated total error).